

## HEAT TRANSFER AND HYDRODYNAMICS IN HEAT EXCHANGERS OF INDEPENDENT ELECTRIC MICROSOURCES (IEM)

Sudarev A.V.\*, Sudarev B.V.

\*Author for correspondence

«Research Center «Ceramic Engines» named after A.M. Boyko»  
Polyustrovsky Av., h. 15, block 2, 195221, St-Petersburg, Russia  
E-mail: [soudarev@boykocenter.spb.ru](mailto:soudarev@boykocenter.spb.ru)

### ABSTRACT

IPMs are increasingly used as power plants (PP) for decentralized energy supply, robotics, transportation, gas pipelines, micro vehicle, etc. applications. IPM's efficiency is ensured by the increased working media initial temperature TIT and the use of efficient miniature air heaters ( $\mu$ AH), which compactness and low material consumption are achieved through the use of some structural materials that do not require cooling at temperatures up to 1350°C, and application of some novel technologies of implementation of **micro channels** in its matrix with the hydraulic diameter of less than 1.5 mm ( $d_h < 1.5$  mm).

The reliability and efficiency of the  $\mu$ AH and gas turbine engine are generally provided at the design stage. This is accomplished using reliable computational relationships repeatedly proven by compact heat exchanger development practice.

Reducing the hydraulic diameter of the micro channel causes a significant reduction in the Reynolds numbers  $Re$  that determine the hydrodynamic flow condition of gas/air in the  $\mu$ AH paths. Condition changing affects their hydraulic resistance and heat exchange intensity. As a rule, micro channels have an arbitrary cross-sectional shape, while the absolute roughness of the walls of any structure is commensurable with the absolute size of their cross section.

In connection with this, for development of a miniature air heater for IPM, it is first necessary to **identify the factors** that have a significant impact on the mass and heat transfer in their micro channels and **to establish the applicability** of the "classical" equations of thermal and hydrodynamic similarity for the thermal hydraulic calculations of  $\mu$ AH.

In this paper, a survey of experimental and theoretical studies on the hydrodynamics and heat transfer in  $\mu$ Cs for  $\mu$ AH and results of the thermal-engineering tests of the metal model of  $\mu$ AH is presented, this  $\mu$ AH having a matrix containing the microchannels of the same dimensions and configuration of the cross-section as are in the matrix of a full-scale  $\mu$ AH.

Analysis of the published material from a number of studies and experimental data obtained on the metal models has shown that "classic" calculation relationships of an acceptable accuracy [1], used for "normal" channels, can also be used for the thermal-hydraulic calculations of  $\mu$ AH.

### INTRODUCTION

It is known that ~30% of the electricity produced in developed countries is spent on the energy supply to houses, public buildings and other structures that do not require mandatory centralized power supply. Each year, the volume of this market segment is growing and increasingly occupied by the decentralized energy supply sources, which serve as a grid support. The decentralization process is driven by frequent natural and man-made disasters, inevitably causing long interruptions in the supply of electricity and heat to thousands of customers.

Usually, power plants are used as stand-alone micro-power and/or mini-sources (IPMs) with internal combustion engines (ICE) or gas turbine engines (GTE) [2] serving as heat engines; use of GTE being thereat preferred due to its lower exhaust emissions. A major shortcoming of the current simple cycle  $\mu$ GTEs is that their efficiency is low due to the scale factor and limited capabilities of heat-resistant metal alloys that do not allow increasing the  $TIT \leq 900^\circ\text{C}$ .

A significant increase in the TIT and, thus, the efficiency, reliability and service life can be achieved using non-shrink structural ceramic materials with high creep rupture strength at temperatures of 1300-1400°C [3]. Even at a high temperature ( $TIT \approx 1350^\circ\text{C}$ ), the miniature gas turbine engine has a very low efficiency ( $\eta_e < (6-8\%)$ ).  $\eta_e$  increasing is achieved through the regeneration of heat, which is realized by incorporating a mini recuperative air heater into the power generation makeup [4] (Fig. 1).

This solution provides a high engine compactness, low mass (3-4 times less that of metal products), and low-cost mass production [2]. We see that the engine compactness is largely determined by the geometrical dimensions of the applied  $\mu$ AH

manufactured using non-shrinkage non-shrinking ceramics [5] and the laser prototyping technology [6]. The  $\mu$ GTE efficiency increase due to regeneration application of various thermal

effectiveness ( $E=70, 80, 90\%$ ) is reflected by the plots, borrowed from the paper by Visser et al [4].

The  $\mu$ AH design concept applicable for the regenerative 2.0 kW engine is shown in Fig. 3.

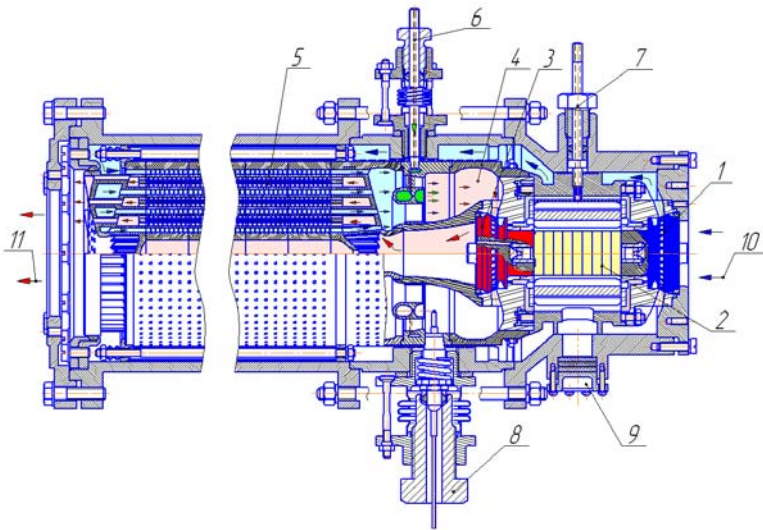


**Figure 1** Miniature regenerative type gas turbine engine with structural ceramics components.

**Designations:** 1 – compressor, 2 – electric generator, 3 – turbine, 4 – combustion chamber, 5 – air heater, 6 – fuel supply, 7 – startup compressed air, 8 – igniter, 9 – electric power removal to customer, 10 – air at compressor inlet, 11 – exhaust gases to be removed to air heater.

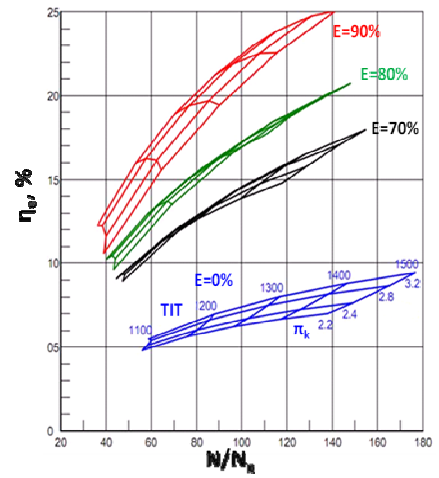


**Figure 2** Effect of regeneration ratio  $E$  on  $\eta_e$  of regenerative miniature gas turbine engine at the rated power  $N_n=3\text{kW}$  at loads  $N/N_n=40-110\%$  [4].

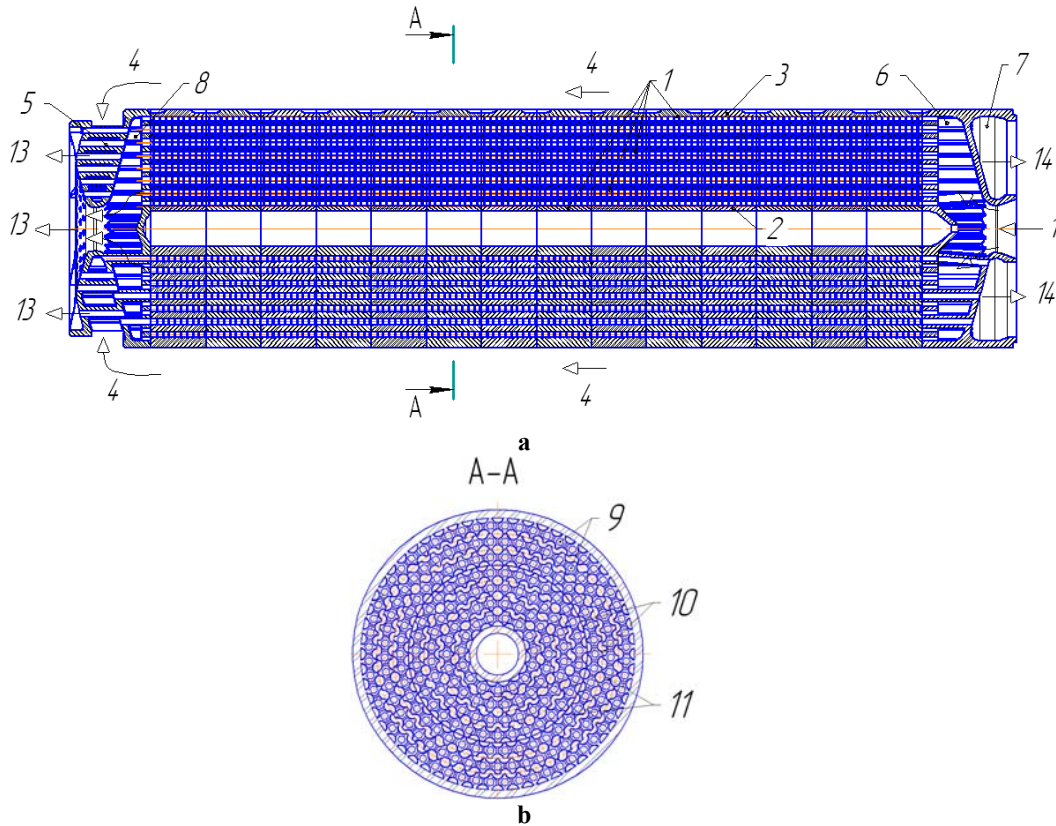


**Figure 3** Longitudinal (a) and cross (b) sections of  $\mu$ AH matrix for regenerative micro gas turbine engine [6].

$\mu$ HP made of structural ceramics is used for heating the compressed air ( $\pi_k=2.5$ ) to a temperature of  $t_a=1,005^\circ\text{C}$  ( $E=0.86$ ) and is intended for use in the "hot" atmosphere at a temperature  $t_g\approx 1,150^\circ\text{C}$ . It consists of a matrix (1), located between the inner (2) and outer (3) shells, the latter (3) of which is separated from the cylindrical body (not shown) of heat exchanger by the annular gap, which serves to move the compressed "cold" air (4) and to provide a counter flow of the working media of microchannels, distribution (5), (6) and collection (7),(8) chambers of these media.

The matrix (1) includes concentric cylindrical shells of uniform thickness and different diameters, where the air (9) micro channels of circular cross section are placed at an equal pitch in the middle of the circle with a cross section, while the gas (10) micro channels of the semicircular cross- cross section and interconnected by the radial (11) micro channels, leveling the distribution of gas over the peripheral gas micro channels in each shell, are placed on the periphery. The direction of the working media flow is indicated by arrows: air (4), (14), gas (12), (13).

To carry out detailed thermal-engineering studies, a metal model (Fig. 4) of  $\mu$ HP is made; its matrix having micro channels of the same cross-sectional configuration and geometrical dimensions as in the full-scale heat exchanger. The difference between the model and full-scale  $\mu$ HP is a number of cylindrical shells that form the matrix. Thus, the model has three shells, while the full-scale heat exchanger has seven shells.



a



b

**Figure 4** Photos of standard sections of matrix (a), general view of metal model of  $\mu$ AH with coolant collection/distribution chambers (b).

The tests of the metal model were carried out at the maximum gas temperature not exceeding  $t_g$ ,  $M<300^\circ\text{C}$ . The results of the model testing are presented in §4.

The careful analysis of experimental and theoretical studies dedicated to identification of the factors that affect the mass and heat transfer in regenerative  $\mu$ AHs was made by Celata G.P. [7]. Authors of the articles quoted in this review note an impact on the hydrodynamics and heat transfer during the motion of gas/air along channels of a small hydraulic diameter ( $d_h<1.5$ ) imposed by such factors as:

- the absolute hydraulic diameter  $d_h$  of the channel;
- the configuration of the cross section and its relative dimensions as applied to the channel of the rectangular section, with width  $b$  and height  $h$  of the channel;
- the relative roughness (RR) of their walls;
- the turbulence ratio at the channel inlet, and, also, the non-stationarity, non-isothermity, flow duty, coolant discontinuity, etc.

Ambiguous and contradictory nature of the mass and heat transfer processes in micro channels, obtained by the studies, is largely due to the difference in processing techniques and the generalization of the experimental data, a different structure of the working areas of the experimental facilities, differing methods of conducting experiments and precision measurements performed.

The results of the experiments show that the empirical correlations developed for the calculation of the coolant flow and heat transfer during the motion of coolants in conventional tubes [1], for which  $d_h\gg\delta_b$  (where  $\delta_b$  is the boundary layer thickness) are not fully applicable to micro channels. It is necessary to carry out a more systematic research to clarify their relation to micro channels.

Celata G.P. [7] notes that some additional mechanisms affecting the formation of boundary layers influence the coolant flow; it is the lack of adhesion of coolant, wall electroviscosity effects, the compressibility of the gas flow, etc.

## 1. HYDRAULIC RESISTANCE AT GAS FLOW ACROSS MICRO CHANNELS

A number of experimental studies reviewed in [8] and dedicated to the microscale thermal hydraulics indicate the presence of significant differences with coolants flowing in micro- and macrochannels, in particular, during the transition from the laminar to the turbulent condition (Table 1).

A detailed review of the hydraulic resistance during the single-phase liquid flow in smooth micro channels with varying cross-sectional configuration and orientation in space, with no heat supply to the liquid, and when it is heated in the laminar, transitional and turbulent duty flows, for media of different viscosities is presented in a comprehensive experimental study by Celata G.P. et al [9]. The authors found that:

- the classical equations of similarity (Hagen-Poiseuille, Blasius) allow to calculate the coefficients of friction with respect to micro channels of any cross-section with the accuracy of  $\pm(10-30)\%$  at various orientations in space, with the hydraulic diameter ranging  $d_h=259-1,699$  microns;
- given the heat supply/heat sink, it is necessary to consider the change in viscosity of the working media.

Table 1

Test findings of studies over hydrodynamics in micro-channels [7-12]

| №  | Tubes, $\mu\text{m}$   | Tube material.<br>Roughness of micro-channel walls  | Coolant                            | $\xi_f$ ; operation<br>range Re  | Transition<br>range<br>Re    | Source |
|----|--|---|------------------------------------|--|------------------------------|--------|
| 1  | 50-254   | Rough channel   | Water                              | $\xi_f \neq \xi_{f,0}$ at low $d_h$ ;<br>$\xi_f \approx \xi_{f,0}$ at high $d_h$       | 300-900;<br>>1,000-<br>1,500 | [8]    |
| 2  | 50-300   | -   | Water                              | $\xi_f < \xi_{f,0}$  | >1,500                       | [8]    |
| 3  | 300-750  | Metal, machined   | Water, methanol                    |  | 700-1,100                    | [8]    |
| 4  | 19;52;102  | -   | Nitrogen; water                    | $\xi_f < \xi_{f,0}$ at laminar<br>duty;<br>250-20,000                                  | 2,000-6,000                  | [8]    |
| 5  | 30-344   | -   | Water                              | $\xi_f = \xi_{f,0}$ ;<br>20-4000   | -                            | [8]    |
| 6  | 320  | -   | Water                              | $\xi_f > \xi_{f,0}$ ;<br>60-600  | -                            | [8]    |
| 7  | 80-166   | Glass, silicon, stainless steel<br>(rough)  | Water                              | $\xi_f = \xi_{f,0}$ smooth<br>tube;<br>$\xi_f \approx 1,15 \xi_{f,0}$ ;<br>rough tube. | 1,700-2,000                  | [8]    |
| 8  | 20-150   | Melted silica   | Water, hexane,<br>isopropanol      | $\xi_f < \xi_{f,0}$ at $d_h < 100$<br>$\xi_{f,\min} = 0,7 \xi_{f,0}$                   | -                            | [8]    |
| 9  | 130  | -   | R114                               | $\xi_f = \xi_{f,0}$ ;<br>at Re < 600;<br>$\xi_f > \xi_{f,0}$ ; Re > 600                | 1,900-2,500                  | [8]    |
| 10 | 760-1090   | -   | water                              |  | -                            | [8]    |
| 11 | 50-254   | Stainless steel; melted silica  | water                              | $\xi_f \neq \xi_{f,0}$ at low $d_h$  | -                            | [9]    |
| 12 | 133-343  | Slot  | water                              | $\xi_f \neq \xi_{f,0}$   | -                            | [9]    |
| 13 | 51-169   | Trapezoidal silicon micro channels  |                                    |  | -                            | [9]    |
| 14 | 50-1120  | Trapezoidal micro channels  | Distilled water                    | Re > 600<br>$\xi_f \approx \xi_{f,0}$  | -                            | [9]    |
| 15 | 15-150   | Stainless steel; melted silica  | Water, methanol,<br>isopropanol    | Re = 8-2,300<br>$\xi_f \approx \xi_{f,0}$  | -                            | [9]    |
| 16 | 26-291   | Trapezoidal silicon micro channels  | Deionized water                    | $\xi_f \approx \xi_{f,0}$ ;<br>laminar duty  | -                            | [9]    |
| 17 | 173-4010   | Tubes   | Air, water, coolant<br>R-134a      | $\xi_f \approx \xi_{f,0}$  | 1,200-3,800                  | [9]    |
| 18 | 50 and more  | -   |                                    | $\xi_f \approx \xi_{f,0}$  | -                            | [9]    |
| 19 | 30 and more;<br>Non-ferrous<br>tubes:<br>848;1237;1699;<br>length 310 mm | Circular tubes, round tubes, all<br>smooth; straight channels<br>( $Ra < 0.1 \mu\text{m}$ );<br>Copper and stainless steel:<br>roughness $Ra < 1 \mu\text{m}$ | Deionized water;<br>coolant R-134a | $\xi_f \approx \xi_{f,0}$  | -                            | [9]    |
| 20 | 310-2,000  | Stainless steel   | Air;<br>$M_{\text{out}} < 0,15$    | Re = $10^3$ - $45 \cdot 10^3$<br>$\xi_f \approx \xi_{f,0}$                             | Re < 2,300<br>[12]           | [10]   |
| 21 | Slotted<br>mounting<br>cooling<br>channels                               | Stainless steel.<br>Smooth slotted channels   | Air                                | Re = $10^3$ - $16 \cdot 10^3$ ;<br>$\xi_f \approx \xi_{f,0}$ ;<br>$\xi_f \neq f(M)$    | Re > 3,500                   | [11]   |

Notes.

 $\xi_{f,0}$  – friction factor, determined by the Hagen-Poiseuille's or Blasius' laws.

Results of the extensive research by Celata et al [9], carried out in 2006, serve as confirmation of the previously (50 years ago, 1956) obtained experimental data for the air flow in capillary channels [10] and in the mounting gaps of

herringbone rotor blade shanks (Fig.5) [11]. These materials have been reported in the well-known monograph by Shvets I.T. and Dyban E.B. dedicated to the air cooling of gas turbines parts [12].

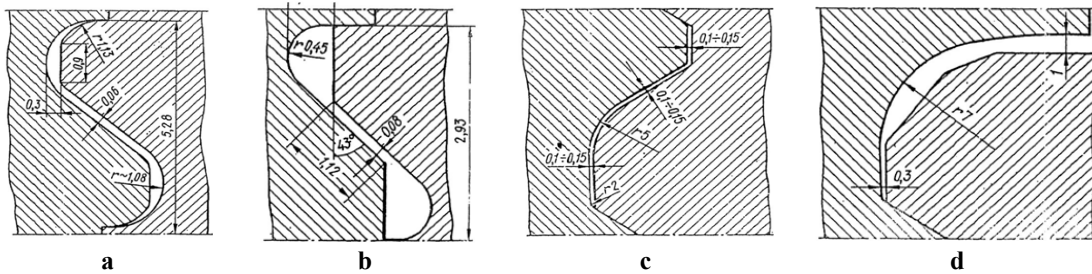


**Figure 5** Mounting gaps and cooling channels for conventional shank joints [12].

**Designations:** a, b – mounting gaps of herringbone GTE shanks; c - the same as before for GT-6-750 by the Turbomotor Works (TMZ); d – cooling channels of shanks for TMZ GT-6-750.

In papers [10-12], it was stated that the air flow in the slotted smooth channels of herringbone shanks is  $\xi_f \approx \xi_{f0}$ . The deviation from the Blasius relation with  $Re=(3-4) 10^3$  does not exceed 15%, while at  $Re=(1-1.9) 10^3$   $\xi_f > \xi_{f0}$  the deviation is 20-40% (Fig. 6-8).

For air,  $\xi_f \neq f(M)$  is up to values of the Mach number  $M=0.9-0.95$ .

The heated air increases the turbulence ratio at the entrance, which leads to an increase in  $\xi_f$ .

At  $Tu > 5-7\%$ , the flow duty is crisis-free.

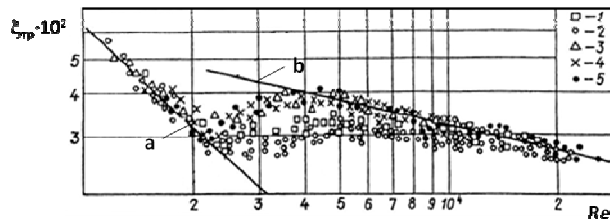


**Figure 6** Relationship  $\xi_f=f(Re)$  for mounting gaps of rotor blade shanks in (1) and b (2), and, also, cylindrical capillary channels of 390 (3); 510  $\mu m$  (4) and 2mm (5) at the adiabatic air flow.

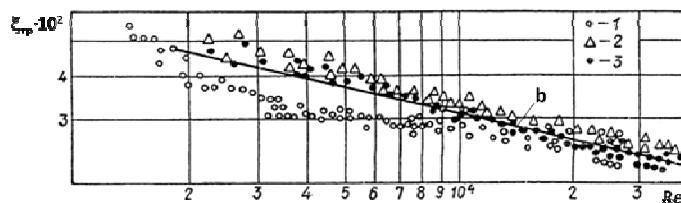


**Figure 7** Relationship  $\xi_f=f(Re)$  for mounting gaps b (1) and cylindrical capillary of 0.51mm diameter (2) and 2mm (3) at the heat supply to air.

At the heat supply to the flow, a smooth (crisis-free) transition from the Poiseuille's relationship to the Blasius' relationship takes place. A similar effect on the patterns of transition is imposed by increasing the level of the initial turbulence  $Tu$  (Fig. 8).

$Tu$  increase reduces the critical Reynolds number of the transition start from 2,300 to  $(1.7-1.8)10^3$  and does not change  $\xi_f$  at the turbulent flow, starting at  $Re > 3,500$ . At  $1,900 > Re > 1,000$ ,  $\xi_f$  is 20-40% higher the value obtained using the Poiseuille relationship.

At the gas flow in micro channels, a number of investigators found out an influence of the compressibility of the gas stream. Guo et al [8] revealed that the change in the gas density in the flow direction can be quite large if the high pressure losses from friction in the flow direction, leading to a change in the velocity profile and friction coefficient  $\xi_f$ , are high (Fig. 9) [13].

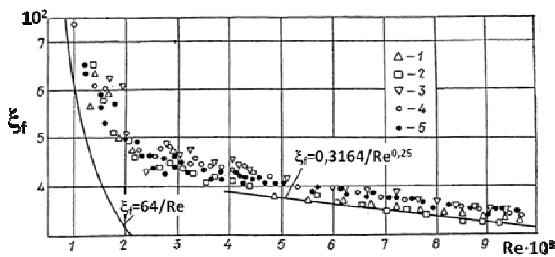


**Figure 8** Relationship  $\xi_f=f(Re)$  for cylindrical channel at various turbulence: 1;2-  $Tu=1-1.5\%$ ; 3;4;5-  $Tu=5-18\%$ .

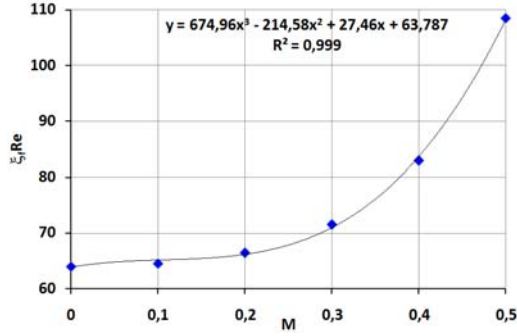


**Figure 9** Effect of Mach number M on the product ( $\xi_f Re$ ) at the laminar gas flow in  $\mu C$  [13].

It is seen that at the gas flow in the microtubes you should not neglect the influence of compressibility. The pressure variations in the gas flow in micro channel can be quite large, while the local Mach number increases with increasing the distance from the entrance, and can become very large even at a low Mach number at the entrance. This phenomenon is critical for the micro systems designing as the **micro channel choking** ( $M=1$  at the channel exit) can occur with the gas flowing even when the input Mach number is much smaller than unity ( $M \ll 1.0$ ). In micro devices, the gas flow velocity is associated with the diameter of the channel by the dependence, varying from cubic to linear, as the flow in the micro channel can vary from the subsonic to the sound value.

$$\xi_f = \xi_{f,0}(1 + M^2 / (1.5 - 0.66M - 1.44M^2)), \quad (1)$$

where M is the local Mach number;

$$\xi_{f,0} = 64 / Re. \quad (2)$$

This conclusion contradicts the experimental data of Shvets I.T., Dyban E.P. [12], and Deych [15], who state that  $\xi_f$  is **essentially independent** of the Mach number (up to  $M=0.9-0.95$ ).

The surface roughness of channels, providing a significant effect on the pressure drop and heat transfer in the micro channels, differs in its structure and the absolute size of the roughness of "conventional" tubes, for which  $d_h \gg \delta_b$ .

However, for micro channels with a non-uniform roughness, as well as for "conventional" tubes, the calculation of the boundary values  $Re_{c,1}$  and  $Re_{c,2}$  can be performed using the formulas given in the handbook by Idelchik I.E. [16], according to which:  $Re_{c,1} = 1,160 (\delta_s/d_h)^{0,11}$  with  $(\delta_s/d_h) > 0.007$ ;  $Re_{c,2} = 2090(\delta_s/d_h)^{0,0636}$  (for tubes with any roughness). In the transition zones of the Reynolds numbers, Celata [8] recommends the following relationship to calculate  $\xi_f$  in  $\mu C$ :

$$Re_0 < Re < Re_{c,1} \quad \xi_f = 4.4 Re^{-0,595} \exp(-0.00275 / (\delta_s/d_h)), \quad (3)$$

where  $Re_0 = 1,900$ ;

$$Re_{c,1} < Re < Re_{c,2} \quad \xi_f = (\xi_{f,2} - \xi_{f,1}) \exp(-(Re_{c,2} - Re)^2) + \xi_{f,1}. \quad (4)$$

Here:

at  $(\delta_s/d_h) \leq 0.007$

$$\xi_{f,1} = 0.032; \quad \xi_{f,2} = 7.244 Re^{-0,643}; \quad (5)$$

at  $(\delta_s/d_h) > 0.007$

$$\xi_{f,1} = 0.0758 - 0.0109 / (\delta_s/d_h)^{0,286}; \quad (6)$$

$$\xi_{f,2} = 0.145 / (\delta_s/d_h)^{-0,244}. \quad (7)$$

At the self-similar turbulent condition,  $\xi_f$  in the micro channels, as in conventional tubes, does not depend on the Reynolds number and is determined solely by the relative roughness value of the channel walls.

For the micro channels in the transition zone,  $\xi_f$  depends on the Re number and the relative roughness; whereas at the transition to the turbulent condition  $\xi_f$  gradually decreases with increasing the Re number, reaching the lowest values of the quadratic (self-similar) mode.

For the laminar flow in the channel with an equivalent relative roughness over 0.7%, the deviation from the Hagen-Poiseuille's law in the direction of increasing  $\xi_f$  is likely to occur. The greater is the relative roughness value, the lower is the Re number, at which the deviation occurs.

Based on the analysis of results of the experiments carried out [9-12], we can conclude that there is no influence of the absolute size of the micro channel in the transition from the laminar to the turbulent flow, which allows to calculate the hydrodynamics in the capillary channels of the criteria relations given in the references [1,16].

## 2. CONVECTIVE HEAT TRANSFER in MICRO CHANNELS

Use of very small diameter channels with their relative length  $(l/d_h) > 100$  leads to the appearance of the laminar flow condition, at which, given relatively low flow rates and hence small values of  $\langle D d_h/l \rangle$  ( $Pe d_h/l < 10$ , where  $Pe = RePr$  is the Peclet number; l is the length of the channel), the Nusselt number Nu ceases to depend on this complex and tends to a constant value  $Nu_{min}$  (Fig.10), that is, the convective heat transfer coefficient is independent of the inertial forces (flow rate of the working media) [17-19].

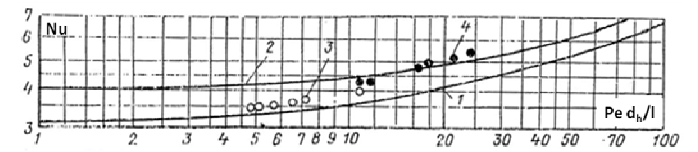


**Figure10** Convective heat transfer in the micro channels under condition  $Pe d_h/l < 10$  for rectangular cross-section channels with various aspect ratio  $\psi = h/b$  (where h, b are thickness and width of the micro channel [17]).

**Designations:** 1,2 -  $\psi=1$ ; 3 calculation; 3,4 -  $\psi=1; 2,62$  - experience [18].

The number  $Nu_{min}$  and the hydraulic resistance coefficient of friction  $\xi_f$  in this case have a significant influence on the cross-sectional shape of the channel. For the capillary tubes of circular cross-section,  $Nu_{min,c} = 3.66$ , and the rectangular  $Nu_{min,r} = 7.5-8.24$  as function of the aspect ratio  $\psi = h/b$ . Here,

$Nu_{min,t}$  is the minimum Nusselt number for the constant wall temperature  $t_w$ . With a decrease in  $\psi$ ,  $Nu_{min,t}$  increases. Reduction of the complex " $Re d_h / l$ " promotes the Prandtl number  $Pr$ , which is less than 1.0 for gas coolants (e.g., air) [17, 19]. With respect to the slotted micro channels, for calculation of  $\xi_f$ ,  $Nu_{min,t}$  you can use the following approximation formulas:

$$\xi_f Re = 57.736 \psi^2 - 95.072 \psi + 94.792; \quad (8)$$

$$Nu_{min,t} = 8.7699 \psi^2 - 13.524 \psi + 7.8092. \quad (9)$$

Under the laminar gas flow in a microchannel (as opposed to the conventional channels [1,12]), the convective heat transfer is significantly affected by the Mach number (Fig. 11) [13].

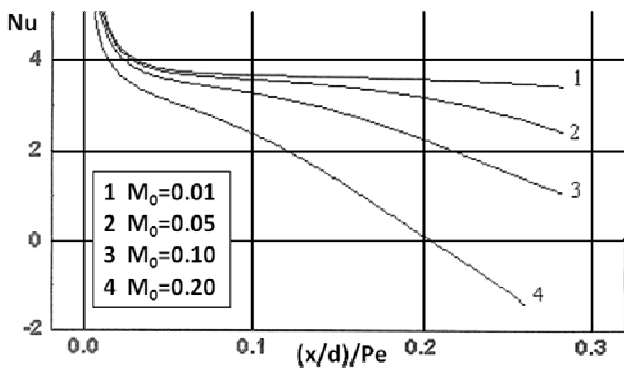


**Figure 11.** Effect of Mach number on the convective heat transfer at gas flow in the micro channels [13].

It is evident that the effect of the Mach number  $M$  on the convective heat transfer in the micro channels is already apparent at  $M > 0.05$  (curve 2), and a situation is likely to occur that the heat flow is directed from the wall to gas, i.e.  $T_{a,w} > T$  (curve 4,  $M=0.2$ ).

$$T_{a,w} = T_g (1 + (r(\kappa-1)/2)M^2), \quad (10)$$

where  $T_{a,w}$  is the adiabatic wall temperature,  $T_g$  is the temperature of the gas flow;  $r$  is the temperature recovery coefficient at the gas flow in the channel, equal to:

$$r = Rr^{0.33} - \Delta r_x. \quad (11)$$

Here:

$$\Delta r_x = 7.16 \cdot 10^5 Re_x^{0.4} f(x/d_h); \quad (12)$$

$x$  is the characteristic size in the Reynolds number;  $f(x/d_h) = 1$  at  $x/d_h = 0-15$  (initial segment);

$$f(x/d_h) = 1 + 0.0413(x/d_h - 15) \text{ at } x/d_h = 15-27 \text{ [15,19]}. \quad (13)$$

The cross-sectional shape of the micro channels is very diverse (Fig. 12). It has a significant effect on the rate of heat transfer in a channel, especially under the laminar condition.

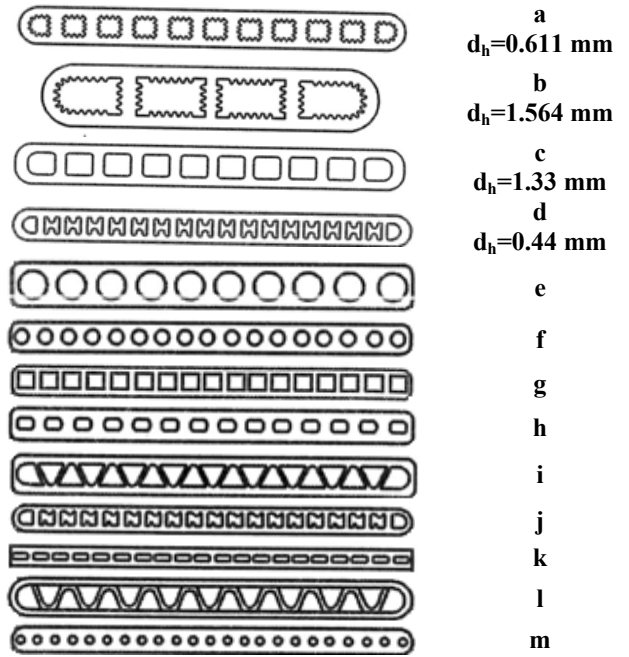


**Figure 12** Shapes and sizes of the cross section of the micro channels in flat multi-channel tubes applied to manufacture miniature heat exchangers [7].

The difference in the convective heat transfer is due to the secondary currents generated in such channels. They lead to significant differences in the heat transfer coefficients in comparison with a circular channel, having the same hydraulic diameter. It is shown in publications devoted to the study of heat transfer in the micro channels ( $d_h < 1.5$  mm) that the technology of manufacture of the test micro channels of a noncircular section causes a number of effects that lead to significant differences in the convective heat transfer, compared with round section micro tubes. The available information on the convective heat transfer in the circular and noncircular micro channels does not provide trustworthy recommendations for the thermo-hydraulic calculations of a compact heat exchangers with micro channels. More systematic researches are needed to consider each of the parameters that affect the transport processes at the gas flow in them. However, it is unacceptable to neglect the experimental information already available, summarized in the paper by Palm and Peng [8] and applying to the heat transfer in noncircular micro channels with  $d_h = 133-367 \mu m$ . They found a significant difference in the intensity between the heat exchange in micro- and "conventional" channels.

At the laminar flow in the micro channels, the test data is generalized by the equations:

$$Nu = C_1 Re^{0.62} Pr^{0.33} \quad (14)$$

or for an array of parallel rectangular channels

$$Nu = 0.1165 Re^{0.62} Pr^{0.33} (d_h/b)^{0.81} (h/b)^{-0.79}, \quad (15)$$

which is applicable at  $900 \geq Re \geq 80$  and  $367 \geq d_h \geq 133 \mu\text{m}$ .

Here,  $C_1$  is the empirical coefficient, which depends both on the hydraulic diameter  $d_h$ , and the ratio of the channel thickness  $h$  to its width  $b$  (Fig. 13).

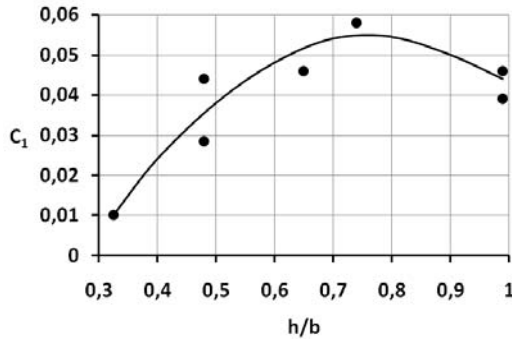


**Figure 13** Effect of the relative height ( $h/b$ ) and  $d_g$  on the convective heat transfer in the micro channels [7].

It is evident that there is an optimal height ( $h/b$ ), which minimizes the thermal resistance in a rectangular channel. In accordance with Peng's experiments, this height is  $h/b \approx 0.75$ .

**Table 2**

Geometries of studied micro channels and empiric coefficient in the criteria equation by Peng [8]

| No | b, mm | h, mm | L, mm | $d_h$ , mm | $h/b$ | $C_1$  |
|----|-------|-------|-------|------------|-------|--------|
| 1  | 0.4   | 0.3   | 50    | 0.343      | 0.75  | 0.058  |
| 2  | 0.3   | 0.3   | 50    | 0.3        | 1.0   | 0.0384 |
| 3  | 0.4   | 0.2   | 50    | 0.267      | 0.50  | 0.0426 |
| 4  | 0.3   | 0.2   | 50    | 0.24       | 0.667 | 0.0472 |
| 5  | 0.2   | 0.2   | 50    | 0.20       | 1.0   | 0.0468 |
| 6  | 0.3   | 0.1   | 50    | 0.15       | 0.333 | 0.0104 |
| 7  | 0.2   | 0.1   | 50    | 0.133      | 0.50  | 0.0285 |

For conditions where  $Re \geq 1,000$ , Peng suggested a correlation  $Nu = C_1 Re^{0.8} Pr^{0.33}$  for the turbulent flow, which, unfortunately, has a considerable scatter of experimental data.

On the basis of the analysis of experimental data on the convective heat transfer in the micro channels under the turbulent flow condition, it was established that for channels with hydraulic diameter  $d_h \approx 1.2$  mm is critical for  $d_h$ , at which you can use "classical" equations of the thermal similarity for calculation of the convective heat transfer [1,16,19].

In Zotov's study [14] over the air flow in slotted microchannels ( $h = 0.048 \dots 0.18$  mm), a stratification of the experimental data, depending on the relative roughness of the channel walls, was revealed despite a relatively small height of the roughness ( $\delta$  less than 1.2 mm). In some experiments, the air stream speed at the outlet of the channels reached the sound level. The results of this work are consistent with the materials reported by Watts [20], which studied the hydraulic resistance of friction  $\xi_f$  at the flow of nitrogen, argon and hydrogen in planar channels of glass and silicone of the height  $h = 0.028 \dots 0.065$  mm, the average height of roughness bumps on

the surface is less than  $\delta = 0.004$  mm, while the relative roughness ratio is  $\Delta = 0.143 \dots 0.0615$ . With such  $\Delta$ , greatly exceeding the limit value  $\Delta_{lim} = 15/Re = 0.03 \dots 0.015$  for any commercially available tubes, stratification should take place, as is noted in the handbook by Idelchik I.E. [16].

Effect of the isotropic roughness on the heat transfer intensity with air ( $R_{sur} = 0.01 \dots 0.7$  MPa) flowing in slotted micro channels is examined in the experimental study [12]. The slotted channels of stainless steel and glass are employed. The absolute roughness of the walls of the channels was  $\delta_s = 0.1; 1; 2; 3; 4; 7; 10$   $\mu\text{m}$ , and the thickness of pads, forming the channel, is  $h = 0.05; 0.06; 0.09$  mm. The pad thickness was measured with the accuracy up to 1  $\mu\text{m}$ . The channel width is  $b = 3.1$  mm, the length is  $L = 13.5; 22.6$  mm. To calculate a slotted length averaged channel  $\xi_f$ , relationship that applies to an object that has no heat exchange with the environment was used, while the resistance coefficient along the length of the channel is constant.

On the basis of the analysis of results of the experiment, we can conclude that there is no influence of the absolute size of the micro channels on the transition from the laminar flow to the turbulent flow, which allows for calculation of the heat exchange in the capillary channels using conventional criteria relations [1,16,19].

All the capillary tubes, where the air flow was investigated [10-12], are hydraulically smooth, so no stratification of the experimental data at the turbulent duty was revealed. Increasing the level of the initial turbulence reduces  $Re_{c1}$  to 1,700...1,800, and practically does not change the friction resistance coefficient in the turbulent air flow.

At a higher turbulence ( $Tu > 5 \dots 7\%$ ), the crisis-free transition from the laminar to the turbulent flow is implemented (Fig. 8), while at  $Re = 1,000 \dots 1,900$ ,  $\xi_f$  is 20...40% higher that calculated by the Hagen-Poiseuille's law  $\xi_f = 64/Re$  for the circular cross-section tubes.

The experimental materials [9-12] confirm the applicability of the classical equations of similarity for calculating the convective heat transfer with gases flowing in the micro channels, and the validity of using the Hagen-Poiseuille's and Blasius' formulas to determine  $\xi_f$ .

### 3. HEAT TRANSFER ENHANCEMENT

To intensify the heat transfer inside the micro channels, some known methods can be used [21], namely the coolant flow twisting [22,23] and the longitudinal channel configuration variation, contributing to the emergence of pressure fluctuations in a moving stream [24-26].

With the gas/air flowing across the curvilinear channel, an uneven distribution of velocities and pressures is established in its sections, transverse pressure gradients emerge, causing a secondary vortex flow that is superimposed on the main stream. The secondary flow lines are locked in the secondary flow channel cross section.

The secondary flow consists of two streams, which are directed to the convex surface near the walls, and in the center of the channel they are directed to the concave surface and have the symmetrical – helical character.

The structure of the secondary flow and the loss of energy, caused by it, depends on the geometrical shape of the channel and the flow condition, defined by the Reynolds numbers and Mach numbers. The secondary flows enhance the heat exchange at any flow mode [22].

At the Dean number,  $De=Re\sqrt{d_h/D_{ben}}=26-7,000$  and  $(d_h/D_{ben})=6.2-62.5$ , where  $D_{ben}$  is the bending diameter, the laminar flow with macro vortices occurs, at which:

$$Nu=0.0575 Re^{0.8} Pr^{0.43} (d_h/D_{ben})^{0.21} (Pr_f/Pr_w)^{0.25} \quad (16)$$

For calculation of  $\xi_f$ , the Tschukin's formula can be used:

$$\xi_f=0.0385(D_{ben}/d_h)^{-5}+0.312Re^{0.25} \quad [22], \quad (17)$$

For the enhancement of the heat transfer, longitudinally profiled tubes with the "convergent-divergent" type configuration were applied. According to the Mighay's data [26], their thermal efficiency at  $Re>10^4$  is significantly higher that achieved by other methods of improving the convective heat transfer in tubes. Systematic experimental studies of the convergent-divergent type models (CDC) and the divergent-convergent channels (DCC), carried out by E.F. Kuznetsov and B.P. Ivanov [25] in a wide range of the Reynolds numbers  $5.0<Re <2\cdot 10^5$ , showed that for some CDC and DCC models within the zone of transition from the laminar to the turbulent flow, a 2.5-3 times growth of the convective heat transfer was obtained with a lagging resistance increase.

#### 4. THERMAL-ENGINEERING TESTS OF METAL MODEL OF $\mu$ AH.

The experimental study of the hydraulic resistance and heat transfer model was made on the experimental setup (Fig. 14), consisting of the working section (1) with a metal model (2) of  $\mu$ AH, supply (3)/outlet (4) "hot" air parts placed on it.

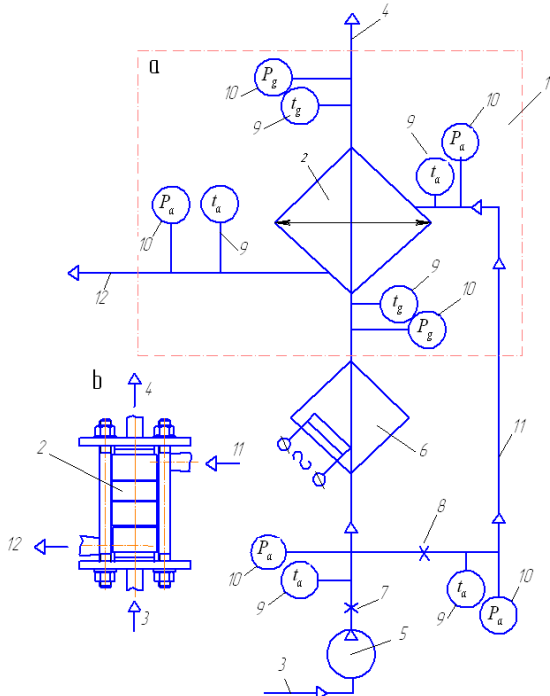


**Figure 14** Schematic diagram (a) of the experimental setup for thermal-engineering test of  $\mu$ AH model (b).

The compressor (5), serving both model paths (2), is placed within the area (3). It is equipped with an electric heater (6), a flow meter (7), pressure gauge (8) and thermal sensors (9), designed to measure the parameters of the gas at the inlet and outlet of the model (within the heat removal area (4)).

The presence of this equipment and instrumentation enables to determine empirically the heat flux released by the "hot" air (gas) in the gas path of the  $\mu$ AH model and to identify pressure losses in it.

The supply (11)/outlet (12) "cold" compressed air has a similar equipment (except for the heater) and instrumentation (8), (9), (10), allowing to determine the heat flux absorbed by the compressed air, and the pressure losses associated with pushing it along the micro channels of the  $\mu$ HP model air paths.

Results of the experimental values of  $Q_g$ ,  $Q_a$ ,  $\Delta p_g$ ,  $\Delta p_a$  in Figure 15 are compared with the calculated  $Q=k\Delta T F$ , where  $Q$  is the heat flux transferred through the heat exchange surface  $F$  of the model matrix,  $k$  is the coefficient of heat transfer, which calculation is performed using the "classical" equation of similarity [1,19],  $\Delta T$  is the mean log temperature head.

The experimental values of the pressure loss  $\Delta p_g$ ,  $\Delta p_a$  in the matrix model paths are compared with calculated values determined using recommendations by I.E. Idelchik [16] for the "conventional" tubes.

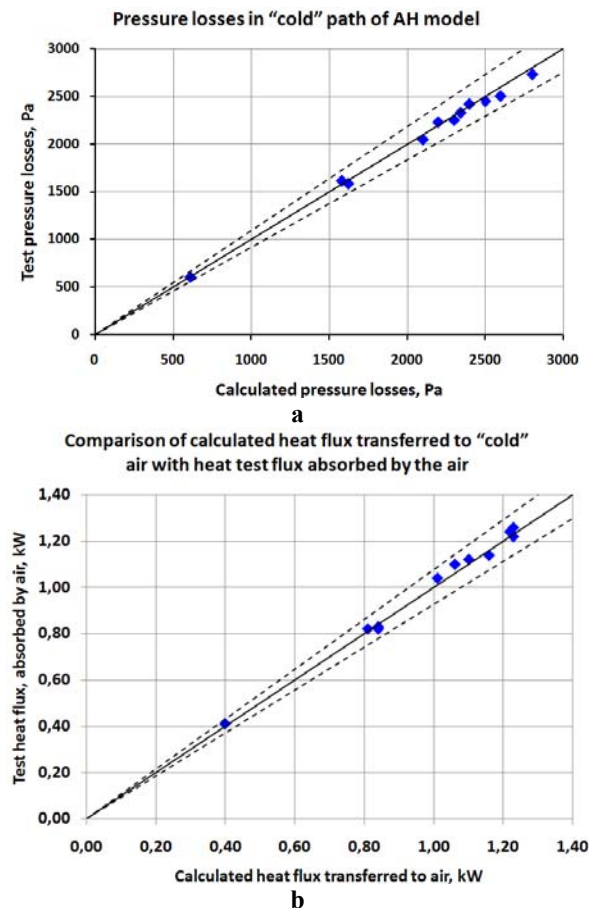


**Figure 15** Comparison of test values  $\Delta p_g$ ,  $\Delta p_a$ ,  $Q_g$ ,  $Q_a$  with calculated  $\Delta p_{g,c}$ ,  $\Delta p_{a,c}$  (a);  $Q$  (b) by recommendations [1;16;19].

## SUMMARY

1. Experimental data on the mass and heat transfer at the coolants flowing in micro channels ( $d_h < 1.5$ ) are ambiguous and often contradictory; they do not provide specific guidance on the thermal hydraulic calculation of miniature heat exchangers, in which matrix similar micro channels are applied.
2. For the thermal - hydraulic design of miniature heat exchangers, it is recommended to use "classical" empirical equations of the thermal and hydrodynamic similarity obtained for "conventional" tubes and channels, for which  $d_h \gg \delta_b$
3. When using "classical" equations of similarity with respect to the micro channels  $d_h < 1.5$  mm, the trustworthiness of the calculated data will be lower than it is the case with "conventional" tubes.
4. Calculation findings obtained using "classical" equations of similarity should be compared with the recommendations of individual researchers, whose empirical equations are placed in this paper.
5. We need to continue research on:
  - a definition of the pressure losses variations in the micro channels,
  - a variation in the density and velocity of the gas/air flows,
  - the Mach number effect on the pressure drop and heat transfer
6. To improve the heat transfer coefficients in both paths of the matrix, channels with slotted or flat-oval cross-sectional configurations should be applied.
7. Reduction of the hydraulic resistance is facilitated using the convergent-divergent type channels.
8. The coolant flow twisting in the  $\mu C$  leads to a significant heat transfer enhancement.
9. Increasing the roughness of the  $\mu C$  walls enhances their hydraulic resistance and will have an insignificant effect on the convective heat transfer due to a total immersion of the roughness bulges in the laminar boundary layer.

## REFERENCES

1. Bazhan P.I., Kanavez G.E., Seliverstov V.M., Reference book on heat exchangers, M.: Mashinostroyeniye, 1989, 366 p.
2. Sudarev A.V., Konakov V.G., High performance green micro source of alternative power supply on the basis of gas turbine ceramic MEMS, 11<sup>th</sup> St-Petersburg International Power Forum, St-Petersburg, Russia, 29 September, 2011, 46 pp.
3. Ghetsov L.B. Materials and strength of gas turbine parts. Book 2, Rybinsk, Pub. «Gas turbine technologies», 2011, 496 p.
4. W.P.J. Visser, S.A. Shakariyants, M. Oostveen, Development of a 3 kW Micro Turbine for CHP Applications, ASME Turbo Expo 2010 Power for Land, Sea and Air, June 14-18 2010, GT 2010-22007, 10 p.
5. Sudarev A.V., Konakov V.G., Morozov N.F., Ovid'ko I.A., Techniques of production of non-shrinkage structural ceramic product, Patent of RF № 2399601 of 19.11.2008.
6. Sudarev A.V., Suryaninov A.A., Ten V.S., Golovkin B.A., Dele A.V., Counter flow plate matrix-circular ceramic recuperator, Patent of RF №2391614 of 10.06.2010.
7. Celata G.P. Heat Transfer and Fluid Flow in Microchannels. New York, Begell House, Inc., 2004, 251 p.
8. Celata G.P., Cumo M., Zummo G., Thermal-hydraulic characteristics of single-phase Flow in Capillary Pipes, Compact Heat Exchangers a Festschrift on the 60<sup>th</sup> Birthday of Ramesh K. Shah, 2002, Pisa, Edizioni ETS, pp. 43-49.
9. Celata G.P., Chmiel K., Kulenovic R., Martin-Callizo C., McPhail S., Mertz R., Owhaib W., Palm B., Sobierska E., Zummo G., Friction pressure drop at single-phase flow in narrow channels, Proceedings of ICNMM2006, 4<sup>th</sup> International Conference on Nanochannels, Microchannels and Minichannels, June 19-21, 2006, Limerick, Ireland, ICNMM2006-96138, 8 p.
10. Shvets I.T., Dyban E.P., Experimental study over hydraulic resistance and heat exchange at the air flow in capillary channels, News of the Academy of Sciences of USSR, Department of Engineering Sciences, 1956, №2, pp.75-82.
11. Shvets I.T., Dyban E.P., Study of the power exchange in mounting clearances of rotor blade shanks, Book 1 «Heat exchange and hydrodynamics», 13, Pub. Academy of Sciences of Ukraine, Kiev, 1956, p. 3-20.
12. Shvets I.T., Dyban E.P., Air cooling of gas turbine parts, Kiev, Naukova dumka, 1974, 488 p.
13. Celata G.P., Cuo Z.Y., Li Z.X., Zummo G., Single-phase liquid flow: effect of gas flow compressibility, Heat Transfer and Fluid Flow in Microchannels, New York, Begell House Inc., 2004, pp. 19-29.
14. Zotov N.M., The experimental heat exchange study at air flow in slotted micro channels, News of High Schools, Mashinostroyeniye, 1969, №8, pp.74-76.
15. Deich M.E., Technical gas dynamics, M., Power, 1974, 592 p.
16. Idelchik I.E., Reference book on hydraulic resistances, M. Mashinostroyeniye, 1975, 559 p.
17. Mighai V.K., Increasing the efficiency of current heat exchangers, L.:LO, Power, 1980, 144 p.
18. Klark S.H., Kays E.M., Transactions of the ASME, Bd.75, 1953, №5.
19. Kutateladze S.S., Basics of heat exchange theory, M.: Atomizdat, 1979, 416 p.
20. Watts J.H., Microturbines: a new Class of Gas Turbine Engine. Global Gas Turbine News, vol. 39; 1999, №1, pp. 4-8.
21. Dreytzer G.A., Current problems of the analysis of efficiency, design, production and running of compact tube heat exchangers, Proceedings of XIII School-Shopwork «Physical basics of experimental and mathematical simulation of gas-dynamics and mass heat transfer in power plants», V. 2, M.: Pub. MEI, 2001, pp.299-306.
22. Tschukin V.K., Heat exchange and hydrodynamics of internal flows in mass forces field, M.: Mashinostroyeniye, 1970, 332 p.
23. Dement'eva K.V., Teleghina I.I., Experimental study of hydrodynamics and heat exchange in curvilinear slotted section channels, Teploenergetika, 1979, №1, pp.51-54.

24. Kirpikov V.A., Orlov V.K., Prihod'ko V.F., Production of compact heat exchange surface on the basis of the concept of introduction of the pressure non-uniformity into current Teploenerghetyka, 1977, №4, pp. 29-33.
25. Ivanov B.P., Kuznetsov E.F., Convective heat transfer and hydraulic resistance of circular variable section channels, Turbines and compressors, 1998, №5, pp.15-21.
26. Mighai V.K., Simulation of heat exchange power hardware, L. Energoatomizdat, LO, 1987, 264 p.